PAPER • **OPEN ACCESS**

A many-body quantum model is proposed as the mechanism responsible for accelerating rates of heat uptake by oceans as anthropogenic heat inputs rise

To cite this article: G B Smith 2024 *J. Phys. Commun.* **8** 115002

Journal of Physics Communications

PAPER

A many-body quantum model is proposed as the mechanism responsible for accelerating rates of heat uptake by oceans as anthropogenic heat inputs rise

G B Smith

School of Mathematical and Physical Sciences, University of Technology Sydney, NSW, Australia

E-mail: geoff.smith@uts.edu.au

Keywords: amplified internal energy, non-thermal energy capacitance, hybrid quanta pairs and refractive index, quantum thermodynamics, information inside heated matter, non equilibrium transitions

OPEN ACCESS

RECEIVED
11 April 2024

REVISED
28 October 2024

ACCEPTED FOR PUBLICATION
5 November 2024

PUBLISHED
13 November 2024

Abstract

A recent many-body quantum approach to thermal radiation (Smith GB, *et al* 2022 *J. Phys. Commun.* **6, 065004**) reveals that the energy capacitance of heated water is about twice its heat capacitance, due to energy stored as local hybrid pairs of photons coupled resonantly to local matter excitations, with pair density weighted by mass density. Energy exchange between photons and localised dipole excitations inside water at steady temperature T, occurs at sites where a hybridisation potential within the Hamiltonian couples local oscillation modes to 'free' photon modes. Photon modes in both directions are phase retarded at exit sides of a hybrid site. Optically sharp variations with frequency in the index of refraction n(f) and photon density of states follow. Exit spectral intensities at equilibrium temperature T carry quantum information on the energy density of matter excitations coupled to photons, while occupied hybrid sites are the source of all 'free' photons and internal spectral intensities. The matter excitations coupled locally to photons are distinct from those that define specific heat, but in water both arise from molecular oscillations. The energy capacitance $C_{EX}(T)$ of hybrid pairs depends on mass density and is independent of the heat capacitance $C_{HT}(T)$, which sets temperature T. $C_{EX}(T)$ is sensitive to T and doubles as a capacitance of energy and of 'quantum information'. Expressions for $C_{EX}(T)$ are derived from first principles and applied to water. The density of occupied hybrids is amplified near surfaces by photons reflected off the surface, which create new hybrid pairs, but not extra heat. Energy capacitance $C_{EX}(T)+C_{HT}(T)$ sets $dT(t)/dt$ prior to a new equilibrium state emerging, after input heating rate dQ/dt is switched. Rising atmospheric intensities then raise T, dQ/dt, $C_{EX}(T)$ and $C_{HT}(T)$. The times available to cool overnight are fixed, so that a rising capacitance, adds to energy stored at an accelerating rate.

Introduction

A concern from global warming is the recent data [1, 2], that shows the heat content and temperature of the ocean is growing at an accelerating rate. The experimental data and quantum thermodynamic models we present in this study show that a second non-thermal contribution to stored internal energy at finite T is present. It is essential to explaining a range of thermal and optical data observable in equilibrium, along with the observed time series $dT(t)/dt$ during the transient non-equilibrium period after a modification of the external heating rate. $dT(t)/dt$ persists until a new equilibrium state and new T stabilise. Adding a non-thermal energy store to existing heat capacitance modifies $dT(t)/dt$ and the total time needed to remove overnight the energy stored during the previous day. The energy stored as heat, is defined by heat capacitance $C_{HT}(T)$, the product of specific heat and mass density of each material, which sets the equilibrium T value. It is made up of quantum thermal excitations, as described in treatments of specific heat in condensed matter physics texts [3]. The experimental data and quantum thermodynamic models we outline and develop in this report show that a second

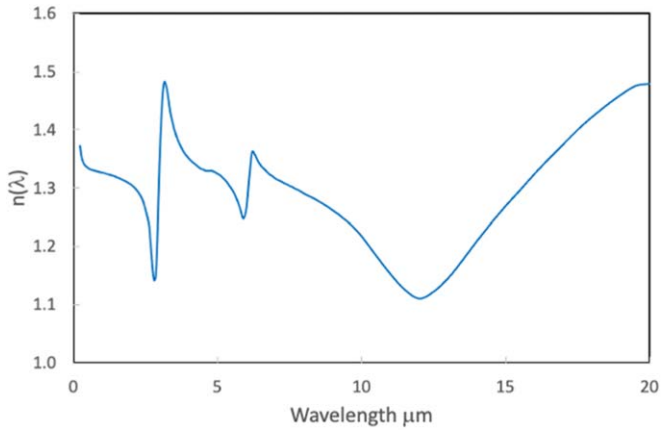

Figure 1. Real part n(λ) of refractive index [n(λ) +ik(λ)] for water [5].

contribution $C_{EX}(T)$, to internal energy stored at equilibrium T is present and is needed to explain a range of thermal and optical observations in equilibrium. It will also impact the time series dT(t)/dt that can be observed during the transient non-equilibrium period after external heating rate dQ/dt is modified. The addition of $C_{EX}(T)$ to $C_{HT}(T)$, extends the transient time-period well beyond what we expect from $C_{HT}(T)$ alone. Past use of observed radiant cooling rates $P_H(T)$ to extract thermal emittance $\varepsilon_H(T)$ [4] of a number of solar selective surfaces did not agree for all samples tested with predictions of loss rate based on $P_H(T) = \varepsilon_H(T)\sigma T^4$, the only model available at that time.

The density of internal photons at each frequency at temperature T represents a third contribution to internal energy density, but as photons have no mass the associated energy capacitance can usually be neglected. Internal optical intensities are expected to be affected by the uniform polarisation they induce in the host material. Optically however the influence of the quantum source of internal photons at finite temperature has unexpected external consequences as optical resonance features are present in emitted optical intensities which are not expected from photons moving along internal ground-state stationary modes defined by a uniform screening potential provided by the polarisation induced in the host. A modification of photon stationary mode densities occurs as the refractive index n(λ) at wavelength λ rises and falls as wavelength λ changes. Examples of n(λ) for water [5], are in figure 1. These variations in n(λ) are sharp and are not characteristic of the dispersion expected from occupied standing wave solutions for 'free' internal photon modes. In the next section we will show that these n(λ) spectral features are due to a sequence of local phase shifts per mode, associated with a series of local resonant delays. We recently showed that since internal photons contributing to internal current density I(f,T) have phase velocities c/n(λ) along each arm of a stationary mode with wavevector $k = n(\lambda)(2\pi/\lambda)$, the number of 'free 'modes up to and including k is $8\pi k^3/3$, so the ground-state mode density depends on $n(\lambda)^3$. As $f = c/\lambda$ the photon density at finite T and I(f,T) both depend on $n(f)^3$ [6]. The quantum physics responsible for these index variations is also responsible for the non-thermal internal energy capacitance $C_{EX}(T)$ within heated matter.

With modelled I(f,T) being sensitive to $n(f)^3$ we demonstrated for water and silica [6] that we could also predict the observed spectral intensities present in emitted intensities by utilising the exit interface transmittance of each I(f,T) incident onto the interface. Example spectral responses had been fitted earlier with arbitrary internal oscillators [7] which happened to also predict observed variations in the infra-red index n(f) [8, 9]. Our models [6] of internal photon energy densities ρ(f,T), which match equilibrium intensities I(f,T) in optically isotropic matter, also predicted the observed optical resonances seen in remotely sensed intensities. The emitted spectral intensities were also found to be duplicating the energy density of select internal matter excitations. The quantum description of how that occurs comes next.

The hybridisation of photon modes with local matter modes

The process in which internal, localised select matter excitations resonantly couple to internal photons leads to a description of the non-thermal energy capacitance. The heat capacitance exists separately. It is induced by external heating rate dQ/dt and has been measured and recorded for many materials. The non-thermal energy component we will show generates mobile photons, which unlike those photons transmitted from externally incident optical radiation sources, including our sun and earth's atmosphere, are not attenuated in equilibrium. It follows that they do not contribute to $C_{HT}(T)$ in equilibrium. 'Free' internally generated optical intensities and their photons are instead phase shifted by their delay at sites where internal photon modes and localised matter

modes are able to hybridise. The resulting local hybrid modes are the ground-state wave solutions of the Hamiltonian whose various potentials include a mixing potential $V_{MIX}(hf,\mathbf{R_j})$ where sites $\mathbf{R_j}$lie along a photon mode at energy hf. Mobile modes coupled to local modes were first studied for noble metal s-band modes coupled to local ionic d-states in dilute alloys [10–12]. Local hybrid coupling of photon modes to matter excitations has qualitative similarity, but the mixing potentials needed are present at high density which must be large enough per mode to generate I(f,T). In equilibrium photon densities at energy hf must also match the densities of their sources in that mode, which are the occupied hybrid sites at T. They relax by emission of photons.

Local hybrid ground-states involving photon modes are predicted by the energy dependent mixing potential $V_{MIX}(f,\mathbf{R_j})$ at site $\mathbf{R_j}$. At finite T in equilibrium many such two-body local states can be occupied at any instant along a single mode, in hf modes in different internal directions, and at many energies hf. The 'free' photons emitted by the next-nearest occupied hybrid state soon enter the neighbour hybrid site. The excitations that can couple at local hybrid sites to photons satisfy new energy and momentum conservation rules, which we will specify later. Other excitations may be present and contributing to the store of heat and the T value. It turns out in ionic solids for example that phonons may be present and contributing to heat gain but not to photon generation. The local excitations in dielectrics that can couple with photons do not propagate and result from anharmonic single polar bond distortions [6]. In most liquids, including water, molecular thermal excitations are local and do not propagate, so they can hybridise with photon modes and if occupied can also emit photons at finite T. When their photon moves on its paired matter excitation relaxes. Maintenance of equilibrium means replacement pairs are being created at a sufficient rate in the same mode at other $\mathbf{R_j}$ to maintain the time-averaged pair density. For water at finite T molecular polar bond oscillations contribute both to stored heat, and to coupling of 'free' photon wave modes to form local hybrid modes. Occupied hybrid states exist in modes in opposite wave directions, which combine to form stationary ground state modes whose wave profiles are adjusted to account for the phase shifts induced by each V_{MIX}.

The quantum fundamentals begin with the addition to the full Hamiltonian of multiple local mixing potentials of the form given in equation (1) whose modes couple free photon modes to matter excitation modes of the same energy. Other potentials present are those that shield photons moving along 'free' mode sections, and those needed to describe matter excitation modes that contribute to $C_{HT}(T)$.

$$H_{MIX}(E) = V_{MIX}(E)c^{*}(E)a(E) + V^{*}_{MIX}(E)a^{*}(E)c(E) \quad (1)$$

Each $c^{*}(E)a(E)$ and its conjugate $a^{*}(E)c(E)$ operate at hybrid sites. The 'free' photon mode densities $\rho(f,T)$ modified by phase shifts are derived from $c^{*}(f)c(f)$ while $a^{*}(f)a(f)$ are the ground state densities of the modes that couple locally to photons. They define energy density $\rho(f,T)$ which becomes a 'virtual density' whose photons are being delayed, so we call such hybrids photonic virtual-bound-states. This many-body model involving multiple local sites for water thus involves in equilibrium an exchange of energy and momentum between photons and local oscillations of water molecules. $V_{MIX}(f)$ enables local optical wave coupling at energy $E_1 = hf$. It is possible that hybrid site occupancy fluctuates between energies hf and 2hf so that mean energy per occupied hybrid site is below 2hf. If that occurs the need for total photon density at hf to match total hybrid energy density per mode does not change and can be met with the addition of extra hybrid sites. A similar problem was found when local valence fluctuations result when two 'ionic' energy levels exchange energy [13]. We will proceed with energy 2hf per occupied hybrid site, though future work may require addition of hybrid sites to yield the required internal total internal optical intensities $I_H(T)$ derived from observed values of $P_H(T) = \varepsilon_H(T)I_H(T)$ if the mean energy content per site is below 2hf.

Pair-forming local excitations can also include oscillations due to anharmonic distortions of bonds in ionic solids [6] as they do not form phonons. Phonons or other extended thermal excitations may be present however and contributing to $U_{HT}(T)$ but are unable to satisfy the exchange conservation rules. Other hybrids in matter involve coupling to localised charge defects such as vacancies and interstitials within non-stoichiometric compounds [14] as found in oxide and nitride based transparent conductors such as ITO [15, 16] and AlTiN [14, 17–19]. A section of a photon mode containing localised hybrid ground states is sketched in figure 2 at finite T. While our focus is the build-up of heat in oceans, models involving hybrid pairs may also impact heat build-up in landscapes. Relevant capacitances are noted in the appendix.

Observations at finite T that are sensitive to hybrid site densities

Measured properties that cannot be explained without invoking local hybrid ground state sites within each photon mode include

- externally measured spectral intensities
- information on matter excitations carried by emitted photons

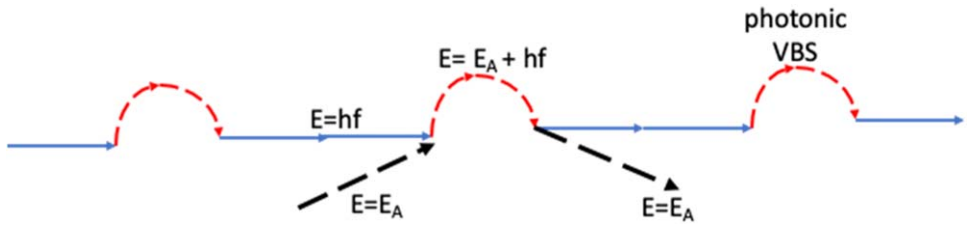

Figure 2. Three adjacent occupied hybrid states formed when a local excitation of energy $E_A = hf$ is stimulated by a photon entering an empty hybrid mode from a 'virtual-free' photon mode. Conservation requires that $E_A = hf$, so each photon-excitation pair energy is $E_{EX} = (2hf)$. When a photon exits its phase $\eta_2(f)$ as it re-enters the adjoining stationary mode has been retarded due to its resonant hybrid delay from $\eta_1(f)$ at entry, and E_A relaxes to zero.

- total internal energy density U(T)
- the rate of change of temperature in the transient period following a change in external heating rate.

Each local excitation and coupled 'free' photon mode have individual occupation probabilities at finite T defined by the Bose–Einstein function $1/\exp[(hf/kT)-1]$. The energy density of occupied local hybrid states at T summed over all energies per site and weighted by hybrid mass density, is both a store of exchange energy $U_{EX}(T)$ and a store of information on each matter excitation energy per hybrid site present at that time. Pairs per site and time-averaged site occupancy are a function of the strength of $V_{MIX}(f)$ and T. They also define the resonant delay experienced by each photon while inside a hybrid site. Total energy density $U_{EX}(T)$ includes all occupied hybrid sites per unit volume, so it is weighted by mass density ρ_m.

The energy capacitance from hybrid pairs is $C_{EX}(T) = dU_{EX}(T)/dT$ which doubles as a store of quantum information on matter excitation energies which are also imprinted onto the exit photons when they leave a hybrid site as an optical phase shift within their exit free mode. Information creation with computers consisting of logic gates has a thermal energy cost [20] as does energy stored by charging arrays of capacitors with an applied voltage. We will show that the non-thermal quantum energy and information capacitance $C_{EX}(T)$ from hybrid pairs is different (the discussion on entropy in the appendix is also relevant). It needs only the finite T value provided by the 'internal heat bath' $C_{HT}(T)$ to exist. At finite T the ground state local and extended waves are activated without doing work. We will evaluate $C_{EX}(T)$ from first principles models of pair density and the energy of each pair. The pair energy density also controls the total density of photons emerging into adjacent 'free' mode sections that link two adjacent hybrid sites, so pair density also defines internal hemispherical intensity $I_H(T)$. This means that $C_{EX}(T)$ and $U_{EX}(T)$ can also be derived from measurements of the hemispherical rate of energy loss $P_H(T)$ from all emitted optical intensities if values of hemispherical transmittance $\tau_H(T)$ are known as radiant intensity $P_H(T) = \tau_H(T)I_H(T)$. $\tau_H(T)$ will be derived using conservation while $P_H(T)$ in equilibrium contains a stable flow of information on matter excitation energies and is not a flow of heat. This model points to ways of controlling the spectral composition within $P_H(T)$, a capability that may be of use in achieving more efficient solar cells. Hybridised modes are also expected in defect free conductors and semiconductors at electron energies nearest to fermi levels, but to simplify this introductory treatment, and for its relevance to ocean heating, we will limit this detailed study to local modal oscillations of polar molecular bonds, using our published models for I(f,T) [6]. We shall show why energy capacitance $C_{EX}(T) = dU_{EX}(T)/dT$ is larger than the heat capacitance $C_{HT}(T)$ for water.

Summing pair energies over all frequencies before weighting with mass density gives total energy density of $2I_H(T)$ with $I_H(T)$ the internal hemispherical intensity if isotropic. The expression for internal energy density $U_{EX}(T)$ in equation (2) includes all such pairs present per unit volume at any instant, and their mass density ρ_m, in the energy capacity $C_{EX}(T) = dU_{EX}(T)/dT$ since

$$U_{EX}(T) = 2I_H(T)\rho_m \text{ Jkg}^{-1}\text{K}^{-1} \tag{2}$$

The information energy capacitance $C_{EX}(T)$ becomes fully 'charged' in equilibrium when the T value set by $U_{HT}(T)$ is stable and T is spatially invariant. In laboratory studies samples of moderate size can be kept at fixed, uniform T. Samples being studied are typically in equilibrium with their local ambient temperature $T_A = T_1$ set by environmental heating rates $dQ(T_A)/dt$. An additional rate dQ/dt leads to $dQ(T_2)/dt$ with T_2 the final steady temperature set by $dQ(T_2)/dt$ such that $dQ(T_2)/dt = [dQ(T_1)/dt + dQ/dt]$. This distinction is important as the study of non-equilibrium transients following a switch in $dQ(T)/dt$ impacts the 'charging rate' of both energy capacitances hence of $dT(t)/dt$, which vanishes in equilibrium. The change in $U_{HT}(T)$ between two steady states and T values once each capacitance is fully charged becomes

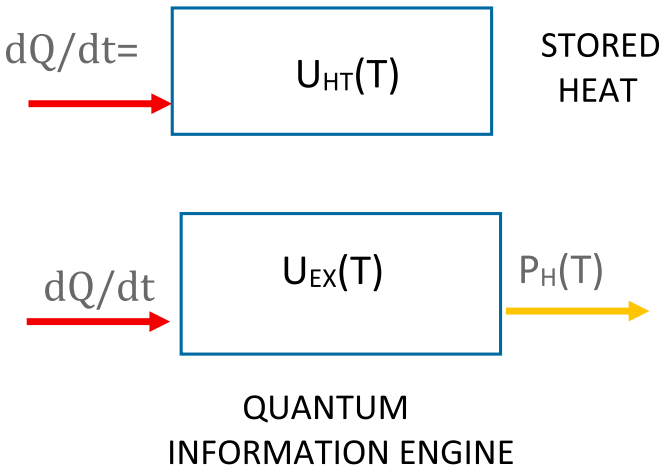

Figure 3. The two parallel quantum capacitances in equilibrium at temperature T have fully charged thermal capacitance. $dU_{EX}(T)/dt = 0$ as its dynamic gains from dQ/dt are in balance with losses from $P_H(T)$, which transports internally gained quantum information to be read externally. Multiple localised hybrid ground state stationary modes are spread along each 'free' photon internal mode as in the small section of one mode shown in figure 2.

$$\int_{T_1}^{T_2} C_{HT}(T)dT = U_{HT}(T_2) - U_{HT}(T_1) \tag{3}$$

Time series data on the values of T(t), dT(t)/dt, and $dP_H(T(t))/dt$ at time t during transients will be useful for fine tuning the fitting of the quantum-thermal model parameters $C_{HT}(T(t))$ and $U_{HT}(T(t))$. For building and environmental heating from solar and sky-based intensities, and for cooling rates at night, transient temperature gradients will often be present along with local fluctuations. They may be observable if sampling times Δt are suitably short. The changes in information capacitance over time Δt during 'charging' and 'discharging' of the heat capacitance can also be expressed in terms of $\Delta T(t)/\Delta t$. Since $C_{EX}[T(t)] = dU_{EX}[T(t)]/dT(t)$ energy and information capacitance charging and discharging rates are $d[U_{EX}(T(t)]/dt = C_{EX}[T(t)]dT(t)/dt$. The quantum expressions following for $U_{EX}(T)$ for the energy contributed by all hybrid pairs present enables evaluation of $C_{EX}(T)$ and time-averaged dT(t)/dt. In equilibrium $U_{HT}(T)$ and $U_{EX}(T)$ are fully charged with heat and occupied hybrid pairs respectively. The input energy flux dQ/dt and exit flux $P_H(T)$ are still present and in balance. Since the energy being emitted at fixed T consists entirely of quantum energy fluxes carrying information, that optical loss of energy is being continually replaced by input dQ/dt at fixed T. We can represent the final steady state as sketched in figure 3.

With parallel quantum energy stores the 'sampling' series $T(\Delta t)$ and $P_H(\Delta t)$ taken over time intervals Δt can provide values of dT(t)/dt after switching to a new dQ(T)/dt. They are modified as shown in equation (4) by the presence of $C_{EX}(T)$. This relation highlights the important impact of $U_{EX}(T)$ and its eventual amplification (that we derive later), on rates of cooling during the transient period from an initial state at T_1 to a final state at T_2.

$$\mp\frac{dT}{dt} = \frac{\frac{dQ}{dt}}{[C_{HT}(T) + C_{EX}(T)]} \tag{4}$$

Cooling rates dT(t)/dt on average overnight and at specific times of day and night and in different geographic locations are important to the environment and to the health of humans, plants, and animals [1, 21, 22]. The impact of $U_{EX}(T)$ and $C_{EX}(T)$ on dT/dt should be known as accurately as possible. Figure 4 provides an overview of charging and discharging dynamics. Climate models need to be adjusted to account for changes in cooling and heating rates relative to what we had expected from $dC_{HT}(T)/dt$ alone. $C_{EX}(T)$ has no net influence on T, except for the time needed for T to stabilise. It has thus aided the long-term thermal stability of earth's environments. That stable situation has now changed due to anthropogenic heating rates as atmospheric radiation continues to rise so that dQ(T)/dt creeps up over time and sets new higher T values.

What appears to create the most impact is the residual store of energy each sunrise (on average over many mornings), due to the slower cooling rates required by equation (4). The outdoor baseline stored heat and energy near ocean surfaces will keep rising. Near surface ocean temperature data [1] also sets radiant power loss $P_H(T)$ but if T has not fully stabilised due to the cooling rates predicted by equation (4) the average energy retained overnight at sunrise will keep rising. It follows that each subsequent average rise in T and dQ(T)/dt will accelerate the mean T values when sampled over sequences of many days or years.

The new models that we previously presented for I(f,T) and 'free' photon densities $\rho(f,T)$ are repeated in equation (5) as they contribute to models of $U_{EX}(T)$ when mass density of their hybrid partner is included.

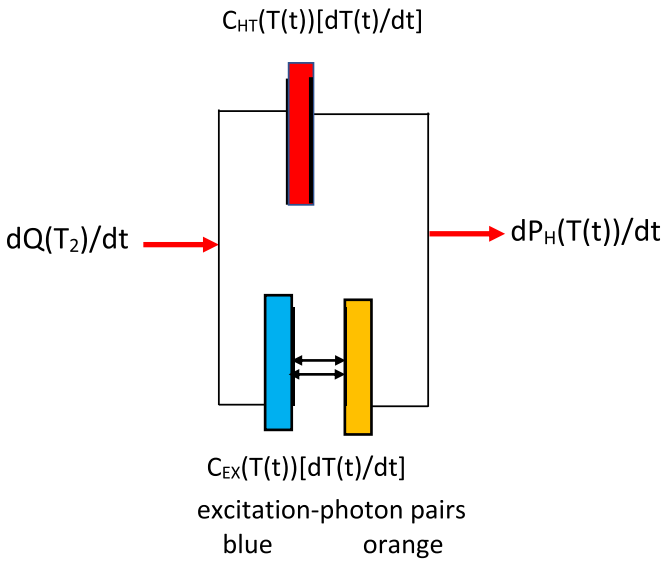

Figure 4. The rate of charging or discharging of both energy stores as a function of the rate of change dT(t)/dt at time t during the period following a switch in the value of $dQ(T_1)/dt$ to a new fixed value $dQ(T_2)/dt$. The heat store, and the information store respond to dT(t)/dt. At T_2 both capacitances are fully charged, and $P_H(T) = dQ(T_2)/dt$.

Observed external spectral intensities cited in that report were qualitatively close to those modelled internally, noting also that exit spectra are now refracted, which led to internal critical angles and total internal reflectance (TIR) for oblique internally incident angles inside still water, above of order 50°. Internal spectral densities are now sample specific as opposed to the reliance on blackbody intensities used by Planck [23–25] to model radiance exiting matter after applying the Kirchhoff rule which does not reproduce the optical transmittance of internally incident intensities [6]. Due to TIR, hemispherical emittance, now given by $\tau_H(T)$, is much reduced relative to Planck-Kirchhoff values as shown later, and tabulated for water. To maintain the familiar historical nomenclature, and to avoid confusion, we will in general use $\varepsilon_H(T)$ in place of $\tau_H(T)$,

$$I(f, T) = \rho(f, T) = \frac{x^3 n(x)^3}{(\exp(x) - 1)} \gamma T^4 = \kappa(f, T) \gamma T^4 \tag{5}$$

$x(f,T) = hf/kT$, $\gamma = 8\pi k^4/(c^3 h^3) = \sigma(15/\pi^4)$ and the spectral property $\kappa(f,T)$ of equation (5) is an alternative and useful spectral parameter at select T values such as 300K, as its values are unique to each material or liquid. The term $n(f)^3$ amplifies the retardation impacts of hybrids within free modes following its lift in optical index to n(f) for photons at T moving along those modes. In many materials a single set of $\kappa(f,T)$ is easily derived over a wide range of T values if optical indices n(f) are known. For water at atmospheric pressure new sets of $\kappa(f,T)$ spectra based on n(f) are plotted in figure 5 and reproduce reported energy density profiles of various oscillation modes [26]. Indices of sea water have been reported only to 25 μm [27] so could not be used, but involve small shifts in n(f) of distilled water.

Remotely collected FTIR spectral intensities from water bodies on Earth and Mars have been reported along with related emissivity spectra on ice and snow [28, 29], with which our predictions on I(f,T) in figure 5 have many common features especially where emitted photon energies peak. Structured interfaces are common on outdoor water or landscape surfaces and tend to wash out spectral features while retaining dominant internal spectral features within I(f,T) (the appendix addresses this). Our I(f,T) spectra for still water given by equation (5) however closely reproduce the molecular excitation spectra of the various oscillation modes in water modelled by Brubach *et al* [26] which track the peaks in n(f) seen figure 1. Published emission intensities from silica near ambient by Wenrich *et al* [7] and from laboratory and remote sensing studies of landscapes rich in silicates [30, 31], plus emission intensities from glazing glass panels used in buildings near ambient, all exhibit sharp resonant spectral intensities between 9 μm to 11 μm, which for silica are predicted accurately with equation (5) [6, 22] with silica n(f).

The link between radiant cooling rate and stored hybrid energy

Summation of $\kappa(f,T)$ over hf and internal elementary solid angles within an arbitrary internal sphere yields the total internal optical intensity $I_H(T)$ of equation (6). Optically derived or experimentally observed $P_H(T)$ is given by $\tau_H(T)I_H(T)$ with $\tau_H(T) = \varepsilon_H(T)$ the hemispherical transmittance. The parameter $\kappa(T)$ introduced in equation (6) is useful to know for the interiors of commonly studied materials, especially for T values near

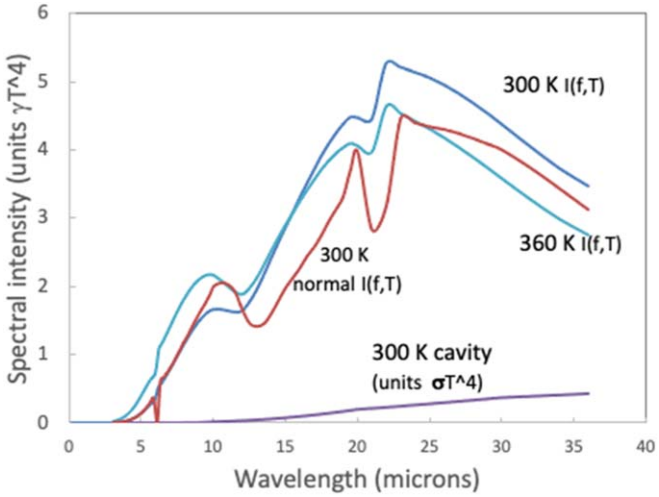

Figure 5. Modelled internal spectral intensity factor κ(f,T) at 300K and 360K within still water. Normally incident internal intensities at 300K (red) are included as they lead to normal exit intensities which are often observed. Cavity internal intensity σT^4 plot is scaled by γ/σ to distinguish it from I(f,T). The molecular resonances within each mode [26] are reproduced when transmittance of I(f,T) $\cos\theta^*$ is observed with θ^* the internal angle of incidence.

ambient. Internal $I_H(T) = \kappa(T)\gamma T^4$ so that

$$P_H(T) = \tau_H(T) I_H(T) = \tau_H(T)\kappa(T)\gamma T^4 \ \ Wm^{-2} \tag{6}$$

This assumes the mean pair energy per occupied hybrid site is 2hf. If it is less than 2hf more occupied sites per unit volume must be present to achieve both $I_H(T)$ and energy

$$U_{EX}(T) = 2\kappa(T)\gamma T^4 \rho_m \ Jkg^{-1}K^{-1} \tag{7}$$

A quick way to establish new $\varepsilon_H(T)$ is to transform past Kirchhoff-Planck (KP) model fits to output power given by $P_H(T) = \varepsilon_{H,KP}(T)\sigma T^4$ with $\varepsilon_{H,KP}(T)$ the hemispherical emittance first introduced by Planck, but based on the Kirchhoff rule. The quantity $\varepsilon_{H,KP}(T)$ arose because Planck assumed that a blackbody term was needed as the internal source for all materials to satisfy the entropy requirements of the 2nd Law. The entropy issue is addressed again in the appendix. External heating 'appears' to have created a drop in entropy, but its creation of $U_H(T)$ provides an internal heat bath at T which allows information creation without doing work. Though it requires T to exist, it is a non-thermal physical store of information. This appears to be contrary to classical expectations, but it is not a paradox in a many-body quantum system. As $\gamma/\sigma = 0.15399$ we can use past fits to accurate experimental studies of $P_H(T)$ to find $\varepsilon_H(T)$ using $\varepsilon_H(T) = 6.49388[\varepsilon_{H,KP}/\kappa(T)]$. For water we calculated using equation (5) and all κ(f,T) that $\kappa(T) \sim 17$, which means at 300K $\varepsilon_H/\varepsilon_{H,KP} \sim 0.382$ so $\varepsilon_H \sim 0.367$. Such low values of hemispherical emittance were anticipated as noted above. A table of $\kappa(T)$ and related parameters for water follows, indicating that water's $\kappa(T)$ is lower than its value in most solid dielectrics, which range up to ~30. What was unexpected but occurs, as we will now prove, is that $I_H(T)$ and $U_{EX}(T)$ have been amplified, as the photons that are internally reflected by an interface within intensity $\rho_H(T)I_H(T)$, with $\rho_H(T)$ the internal hemispherical reflectance, generate additional hybrid pairs.

The remaining theory proves that the amplification factor is $1/\varepsilon_H(T)$ so that low values of $\varepsilon_H(T)$ have high significance, as they will further slow cooling and heating rates by raising $U_{EX}(T)$. At the same time the large internal gain in photon and pair density has no impact on $P_H(T)$ since the gain is cancelled when $\varepsilon_H(T)I_H(T)$ is evaluated which ensures that $P_H(T) = dQ/dt$. The full proof is as follows. Conservation of total energy and momentum requires that $\rho_H(T)I_H(T)+\tau_H(T)I_H(T) = I_H(T)$, or in concise form the conservation rule for total energy and momentum flows at the interface is

$$\rho_H(T) + \varepsilon_H(T) = 1 \tag{8}$$

$I_H(T)$ consists of all the 'free' photons moving in one hemispherical direction and propagating within uniform internal intensities I(f,T), whose free photons are propagating after exiting a local occupied hybrid state. The 'free' photons in any internal intensity resulting from hybrid exit in equilibrium are in effect not attenuated as any internal loss is apparent only, as it occurs when they enter a hybrid mode from which they eventually remerge. The same balance occurs for photons that are internally reflected upon impact with the interface. Temperature in equilibrium is controlled by $C_{HT}(T)$, so does not vary. $C_{EX}(T)$ however is amplified as internally reflected photons have generated extra coupled pairs at fixed T upon entering local empty hybrid mode sites within a photon mode. The values of $U_{EX}(T)$ and $I_H(T)$ when photon recycling is neglected are important and have role to play, especially in practice at distances well away from an interface. For them $U_{EX}(T) = U_{EX}(T)_0$ and

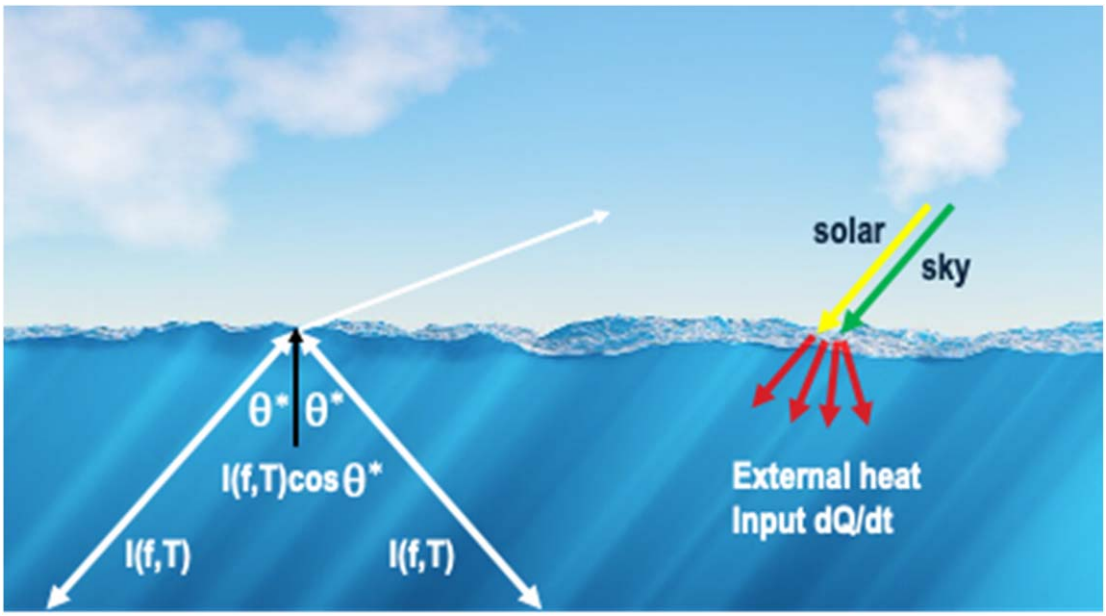

Figure 6. Examples of spectral intensities produced internally and then amplified by internally reflected photons (white). The photons transmitted from each incident I(f,T) are refracted while reflectance is subject to the internal critical angle θ_C^* at each frequency. The intensities I(f,T) flow in both directions and fill a hemisphere at each frequency. They experience no net attenuation unlike like those from environmental external sources shown on the right. The (white) intensities are amplified in equilibrium due to reflected photons generating new hybrid pairs.

$I_H(T) = I_H(T)_0$. Recycling based amplification can in principle impact to large distances from an interface but density variations in the host or impurity content changes with depth, as occurs in seawater, can refract, scatter or annihilate hybrid sourced photons. In thick, deep environmental bodies normal thermal diffusion will occur but direct pair diffusion may be unlikely as each new local hybrid excitation has to be either photon or temperature driven so we expect that at depth values of $U_{EX}(T)_0$ and $I_H(T)_0$ will occur but be dropping as T falls as seen in known data on T as a function of depth [1]. In the case of oceans, these temperature profiles are being measured at some locations over extended time periods, so in zones well below the surface at decreasing T values photons and pairs will be present, but with energy densities close to $U_{EX}(T)_0$ if recycling impacts are absent far down as expected.

Near surface equilibrium temperatures are most important as they dictate radiant power loss $P_H(T)$ to the atmosphere and to outer space[22]. The amplification of internal intensities from photon initial internal recycling followed by secondary and higher order generation of hybrid pairs we will represent by $I_H(T)/I_H(T)_0$ with $I_H(T)_0$ the uniform intensity in equilibrium in the absence of photon recycling. We will also see that transmittance of $I_H(T)_0$ after projection onto the interface of all $I(f,T)_0$ from equation (5) as shown in figure 6, also leads to the observed value of $P_H(T)$. The self-consistent relationship connecting $I_H(T)_0$ to $I_H(T)$ after addition of $\rho_H(T)I_H(T)$ is

$$I_H(T)_0 + \rho_H(T)I_H(T) = I_H(T) \tag{8a}$$

For the oceans the source of dQ/dt and examples of total internal intensities including those resulting from internal reflectance are sketched in figure 6. Internal spectral intensity I(f,T) is the same in all internal directions in optically isotropic matter, and its transmitted intensities are refracted. Absorption of incident solar and atmospheric radiation defines external heating rate dQ/dt. Internally reflected photons from all I(f,T) do not add additional heat in equilibrium as just explained. Initial $I(f,T)_0$ are uniform in all directions and in equilibrium we expect uniformity, even after amplification. Eventually scattering or chemical and density defects will lead to $I(f,T)_0$ at deeper depths where stable measured T values are the result of diffusion from gradients in T value, plus mixing by pressure gradients, currents, and trade winds [32]. Returning to equation (8) and solving for $I_H(T)$ yields equation (9), once the conservation and probability rule of equation (5), written as $[1- \rho_H(T)] = \varepsilon_H(T)$ is applied. Then

$$I_H(T) = \frac{I_H(T)_0}{[1 - \rho_H(T)]} = \frac{I_H(T)_0}{\varepsilon_H(T)} \tag{9}$$

The free photon energy density is defined by the energy density of the photon pairs as they are the source of internal photons. From equation (9) with $P_H(T) = \varepsilon_H(T)I_H(T)$, $I_H(T)_0 = dQ/dt$ and $I_H(T) = I_H(T)_0/\varepsilon_H(T)$ then

Table 1. The parameters that define stored energy and stored quantum information within water in thermal equilibrium at 300K. Each energy capacitance is in units of $Jkg^{-1}K^{-1}$.

Properties at 300 K	Water
$\kappa(T)$	17
$\varepsilon_{H,KP}$	0.95
τ_H or ε_H	0.363
Amplification factor $1/\varepsilon_H$	2.76
$C_{EX}(T)_0$	3,210
$C_{HT}(T)$	4,200
$C_{EX}(T)$	8,850
$C(T) = C_{HT}(T) + C_{EX}(T)$	13,050
$C_{EX}(T)/C_{HT}(T)$	2.10
Mass density kgm^{-3}	998

$P_H(T) = I_H(T)_0 = dQ/dt$, as required externally. That is, had we just relied on external observation of emitted optical intensities from a sample with uniform T to establish pair densities, the resulting energy contribution would be much lower than it is when modified by near surface amplification. In equilibrium balance must exist between the extra photons entering and leaving local hybrid modes following internal reflectance as it does for those making up $I_H(T)_0$. Key parameter values will be tabulated from these models that can be extracted from optical and thermal observations in equilibrium, along with modelled capacitance values that set dT/dt and the time needed for a new equilibrium state to emerge near surfaces. The equilibration times needed are increasing due to ongoing increases in the atmospheric radiation intensities that impact the oceans and produce slowly rising dQ/dt and T, especially at night and early in the morning. The acceleration in the rates that near surface T values are increasing in the ocean can be attributed in the long term to slower cooling rates from a continuing increase in the value of C(T) magnified by gains in $C_{EX}(T)$ from photon recycling.

The amount of quantum information stored in equilibrium is governed by $U_{EX}(T)$, as defined by the store of many pairs of photons coupled at many sites in volume V to matter excitations. The time spent by each photon and its matter excitation partner at each hybrid site depends on the value of the strength of hybridisation given $V_{MIX}(hf)V_{MIX}^*(hf)$. Labelling $U_{EX}^*(T)$ as the hidden energy content in units of $Jkg^{-1}K^{-1}$ we have $U_{EX}^*(T) = (U_{EX}(T)\text{-}U_{EX}(T)_0)$. Setting $U_{EX}(T)/2\rho_m = I_H(T)$ in which $U_{EX}(T)_0$ and $I_H(T)_0$ are both amplified by $1/\varepsilon_H(T)$, means there are no external observable impacts of $U_{EX}^*(T)$ in equilibrium. That means the equilibrium data that can be modelled using values of n(f), c/n(f), T and $P_H(T)$ does not include the internal amplification needed to model $U_{EX}(T)$. So amplification has no measurable external impact in equilibrium. It does however have an important influence during non-equilibrium periods where the time series dT(t)/dt due to C(T(t)) at times t when applying equation (4) after a new dQ(T)/dt value has been switched on. During the transient period capacitances $C_{HT}[T(t)]$ and $C_{EX}[T(t)]$ are partially charged while dT(t)/dt and $P_H[T(t)]$ are varying. That means there are two sets of time series data that can be observed and used to test these capacitance models, especially the modelled equilibrium values of $C_{EX}(T)$.

A table follows for the model's parameters for still water. It includes values for $U_{EX}(T)_0$, and the fully charged $U_{EX}(T)$ value including its amplification. In place of a direct comparison of $U_{EX}(T)$ to $U_{HT}(T)$, we compare heat capacitance $C_{HT}(T)$ with the pair capacitance $C_{EX}(T)$. Heat capacitance and associated specific heat data, feature in many well-established databases of thermal properties. Relevant data on solids was acquired in our laboratory, with a special FTIR optical set-up with a goniometer. Though unsuited to use with water that system produced external reflectance values of total emission from solids which led to KP values of emittance at that time, and for some samples 2-d colour maps of intensity versus direction and wavelength. Results on nanostructured surfaces acquired with that system have been published and are of interest to specific applications [33, 34]. At that time the Planck-Kirchhoff formulation using the spectral algorithm involving blackbody spectral weighting for each exit intensity was applied. Such emissivity values can now also be scaled with $\kappa(f,T)$ to find $\varepsilon(f,T)$ then $\varepsilon_H(T)$ using $\kappa(T)$. We did that for the scaled water results in table 1 based on summation of $\kappa(f,T)$ to establish $\kappa(T)$. External intensities can be found using internal spectral transmittance acting on $I(f,T)\cos\theta^*$ with $I(f,T) = \kappa(f,T)\gamma T^4$ of equation (5). $\kappa(f,T)$ was modelled for water, using its n(f) values with equation (5). We also used hemispherical intensity data acquired by Sasaki *et al* [35] and our modelled $\kappa(T)$ values with equations (2) and (6) at 300K to test the model's optical predictions. For the tabulated pair energy capacitance, we used the expression $C_{EX}(T) = dU_{EX}(T)/dT$ in the sequence given in equations (10) and (11) that starts with $C_{EX}(T)_0$. For $C_{HT}(T)$ published values at 300K were taken from already cited papers and databases.

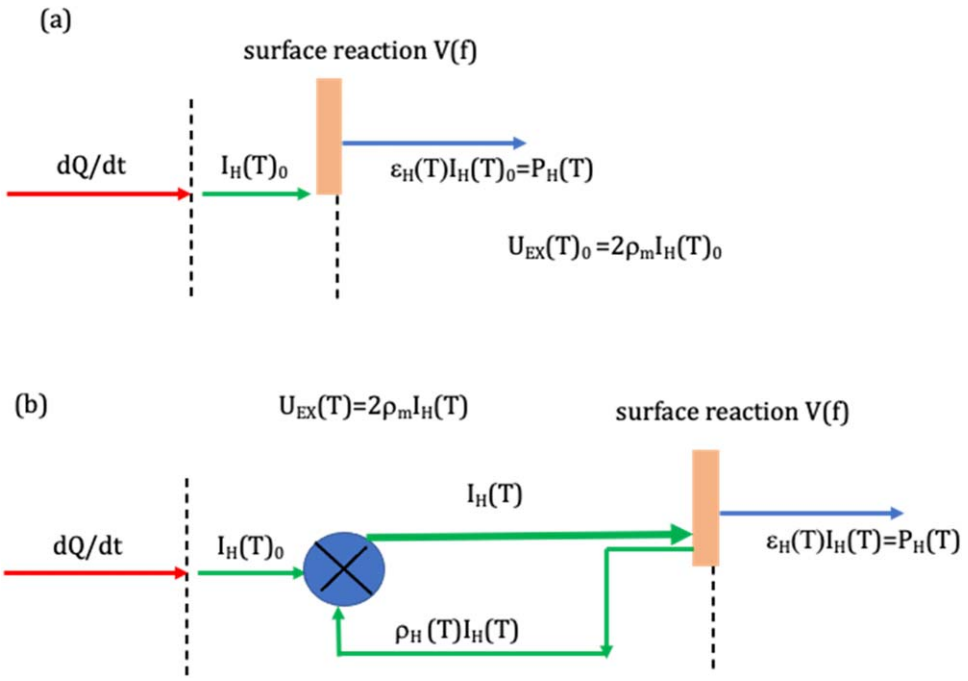

Figure 7. Internal hemispherical optical intensities and the energy densities from the localised exchange-coupled pairs that supply internal 'free' intensities. (a) neglect of photon recycling (b) with photon recycling. They can be derived from experimental values of dQ/dt or $P_H(T)$ or modelled separately starting from local hybrid sites per mode when occupied at finite T. Vertical dashed lines define the interface location where a reaction potential V(f) (orange) acts on incident photons, some of which tunnel through, others are recycled. $C_{HT}(T)$ is present but not shown.

$$C_{EX}(T)_0 = 2\rho_m \frac{d}{dT}(\kappa(T)\gamma T^4)$$
$$= 2\rho_m \gamma T^3[4\kappa(T) + T(d\kappa(T)/dT)] \quad (10)$$

$$C_{EX}(T) = \frac{C_{EX}(T)_0}{\varepsilon_H(T)} \quad (11)$$

Heat and information capacitance values each include the mass density of sample material. $d\kappa(T)/dT$ in equation (10) changes slowly as T varies near ambient so for changes in temperature near 300K we set $d\kappa(T)/dT = 0$ and the T^4 term dominates. The values in table 1 thus arose from $C_{EX}(T)_0 = dU_{EX}(T)_0/dT = 8\rho_m\kappa(T)\gamma T^3$ and $C_{EX}(T) = C_{EX}(T)_0/\varepsilon_H(T)$. The heat capacitance $C_{HT}(T)$ at 300K uses existing experimental specific heat and mass density. The free photon energy capacitance is present but not included as it is $\sim 10^{-3}$ times $C_{EX}(T)_0$.

Results and conclusions

Figure 6 details the energy fluxes and stored energy with $I_H(T)_0$ found by fitting measured $P_H(T) = \varepsilon_H(T)I_H(T)_0$ using known n(f) to fix $\kappa(T)$ so that $\varepsilon_H(T) = 6\square 49388[\varepsilon_{H,KP}/\kappa(T)]$ from past fitted values of $\varepsilon_{H,KP}(T)$. The $I_H(T)$ in figure 7(b) arises from the internal photon intensity (in green) which includes the consequences of the feedback of photons given by $\rho_H(T)I_H(T)$. A large gain in $C_{EX}(T)$ and $U_{EX}(T)$ results as exemplified in table 1. These gains apply only to $C_{EX}(T)$ and $U_{EX}(T)$, as $C_{HT}(T)$ is not affected by the recycling of photons in equilibrium. The existence of an internal many-body-energy term made up of hybrid pairs, enabled us to explain the presence of quantum information on matter excitations being carried by emitted photons at each energy hf. The total emitted intensity $P_H(T)$ at fixed heating rate carries that information despite the preservation of the identity $P_H(T) = dQ(T)/dt$. The parameter values in table 1 relied on the need to maintain consistency of observed optical intensities and those based on electromagnetic models with the predictions of the fluxes in parallel internal and external modes. The surface reaction potentials sketched in figures 7(a) and (b) are present in the Hamiltonian and are implicit in the use of optical reflectance and transmittance to establish transmittance and reflectance of I(f,T) and $I_H(T)$ at the interface.

The physical description of table 1 parameters

$\kappa(T)$, the sum of internal 'free' photon spectral densities in equilibrium

$C_{EX}(T)_0$, the energy capacitance from hybrid pairs derived from $P_H(T)$ data

$C_{HT}(T)$, the measured and theoretical heat capacitance defined by $dU_H(T)/dT$
$C_{EX}(T)$ the amplified energy capacitance $C_{EX}(T)_0/\varepsilon_H(T)$ after internal reflectance
$dU_{EX}(T)_0/dT = C_{EX}(T)_0 = 8\gamma T^3\kappa(T)$ and $C_{EX}(T) = 8\gamma T^3\kappa(T)/\varepsilon_H$

The equilibrium 'hidden' energy $U_{EX}{}^*(T)$ and its 'hidden' quantum information cannot be observed or evaluated from observed external loss rates $P_H(T)$, but can be calculated from optical data using equation (12) plus the amplification factor defined in equation (9)

$$U^*_{EX}(T) = 2\rho_H(T)\rho_m[I_H(T) - I_H(T)_0]$$
$$= 2\rho_H(T)\rho_m P_H(T)\left[\frac{1}{\varepsilon_H(T)} - 1\right] \text{Jkg}^{-1}\text{K}^{-1} \quad (12)$$

The 'hidden' energy is thus a significant multiple of $U_{EX}(T)_0$ in table 1. The amplification factors $1/\varepsilon_H(T)$ for water in table 1 is of order 2.7. These models predict amplification is higher in most dielectric solids. Minor corrections to our gain values may be needed as the full range of indices n(f) were not always available. ε_H derived from past experimental values of $\varepsilon_{H,KP}(T)$ at T near ambient should be reliable if $\kappa(T)$ is accurate, and can also be cross- checked against values of ε_H found by other methods [34].

Hybrid, localised quantum states formed between extended waves and local matter modes are playing an important role in these quantum thermodynamic systems by allowing information creation to occur within heated matter. That store of information adds considerable energy capacitance to the capacitance evaluated from specific heat and it occurs across a wide range of temperatures. Future research should include novel experiments and theory to explore and test the models introduced in this paper in terms of their impact on the values of the extra energy capacitance. Studies of the role of sample size, shape and interface structures are needed to refine and expand the models this paper has introduced. Our current models for the thermal responses of built and natural outdoor systems irradiated by solar energy during the day and atmospheric radiation for 24 h may need refining. For buildings roofs, walls, and windows estimates of T, d[T(t)]/dt and stored energy can be refined for improved comfort, less use of supplied energy, and better human, plant and animal health in a warming climate. The reduced rate of cooling overnight from the large increase in near-surface energy capacitance we propose is the source of accelerating temperatures in our oceans. The impact of ongoing rises in greenhouse gas densities in our atmosphere plus the amplification of $C_{EX}(T)$ by internal photon recycling by ocean surfaces need inclusion in climate models.

Acknowledgments

Dr A Gentle designed and constructed our FTIR systems. He is now in the PV group at UNSW. He also provided useful criticisms on the early drafts of this paper. Prof Matt Arnold and Dr Gentle both contributed to reference 6, which focussed on emitted spectral intensities and had to be refined for this study.

Data availability statement

All data that support the findings of this study are included within the article (and any supplementary files).

Appendix

The absence of heat generation by internally generated photons

It is usual to assume that photons making up optical intensities within absorbing matter are nearly all annihilated after travelling distances $d^*(f)$ of a few mean-free-paths per mode where $\langle d^*(f)\rangle = 1/\alpha(f)$ and $\alpha(f)$ is the absorption coefficient per mode. That applies to intensities from external optical sources. Intensities sourced and produced internally consist of photon fluxes within multiple parallel modes at energy hf and can be extracted from external optical data acquired with spectrophotometers or indices found with ellipsometers. At finite T the 'free' photon modes and intensities I(f,T) generated internally when modes are occupied, have undergone many phase shifts due to photon delay at hybrid sites while coupled to local matter excitations. The delay introduced by the hybridising potentials $V_{MIX}(hf)$ in each direction modifies the stationary wave formed from each 'free' mode for waves in opposite direction. In equilibrium any loss as heat would need to be compensated by a loss of an existing $C_{HT}(T)$ excitation and an addition of a new $C_{EX}(T)$ pair so the time-averaged densities of hybrid pairs and photons remains in balance. Photons entering a hybrid site are not lost as discussed as they remerge so that those between hybrid sites and those at hybrid sites are in dynamic balance.

With $\langle d(f)\rangle = 1/\alpha(f)$ [6] for photons incident externally that generate a stable value of heating rate $dQ(T)/dt$ in equilibrium, solar heating of outdoor surfaces results. Internal energy density now has two components, the

thermally excited multiple single quanta that are excited by dQ/dt and charge $C_{HT}(T)$, and the many sets of paired quanta that exist at T and charge $C_{EX}(T)$, which generates the internal photons that occupy each I(f,T) that can be projected obliquely onto the exit interface. Oblique internal reflectance and external transmittance (which we previously called emissivity) are sensitive to polarisation, which means the gain from formation of additional hybrid sites induced by reflected photons is also polarisation dependent.

Surface profiles and emittance

The differences between $\varepsilon_H(T)$ the new hemispherical transmittance and $\rho_H(T)$ are influenced by surface structure, whether by its contours, porosity, or nanostructure. The ratio of $\rho_H(T)$ to $\varepsilon_H(T)$ has a strong influence on the amplification of information energy capacitance in the vicinity of the interface to depths where the first generations of hybrid pairs continue to form without optical loss. That will in practice change when any non-uniformity exists whether from defects, impurities or host density variations which induce losses by scattering and absorption. Momentum conservation is now included in these models and is different for each different surface profile but is present in all $\rho_H(T)$. Its impacts internally and externally on emitted intensities can be modelled or simulated for many exit profiles. In general, any surface that reduces $\rho_H(T)$, will also raise $\varepsilon_H(T)$ and reduce $I_H(T)$ and $C_{EX}(T)$. A porous or rough interface will do this.

Entropy S(T)

Entropy flux $S(T)_{EX}$ relates to probabilities that hybrid sites at different energies will be occupied at T which is set by their distribution among available hybrid ground states at each energy 2hf and temperature T. No external work is done by the internal quantum engines that transform external heating rate dQ/dt into internal optical intensities carrying quantum information on those matter excitations that photons couple to at hybrid sites. The stored heat in $U_{HT}(T)$ could in principle be used to do some external work but if that happened equilibrium $U_{EX}(T)$, $U_{HT}(T)$ and T would all fall but information within the reduced $U_{EX}(T)$ would still be present. The excited hybrid pairs are non-thermal quanta, carrying information, and the 'free' photons they internally emit are not sourced from the thermal store. Ceasing the practice of 'labelling' of exit intensities with the words 'thermal' or 'thermal radiation' might aid the understanding of what this 'energy' represents. Information bearing radiation reinforces the observed reality that $P_H(T)$ is transporting quantum information on those matter excitations that resonantly co-exist with photons at sites where hybrid modes exist.

$\Delta U(T)$ when T is changed in steps remains associated with $\Delta S(T) = \Delta U(T)/T$. Energy is however flowing into and out of the non-thermal energy store at equal rates isothermally in equilibrium as in figures 3 and 4, when $U_{HT}(T)$ is in a fully charged state. This means there is no net change to entropy when the multiple two-body quanta present at finite T internally emit those photons which escape as external energy flows. These energy and information creation issues are not covered by the Landauer postulate applied to information generated by computer circuits, nor by invoking Maxwell demons of quantum particles embedded within an internal thermal environment which have been briefly addressed [36]. Collections of many-body local hybrid excitations enable photons residing at each site during resonance to 'pick-up' quantum information on its matter partner. Upon internal exit as a 'modulated' photon, it can either be internally recycled or contribute to $P_H(T)$. The net result for entropy change from input of dQ/dt to output of $P_H(T)$ is that $\Delta S(T) = 0$ and the full cycle is reversible. In terms of the 2nd Law this information only 'appears' to be produced by external heating. It exists whenever T is finite and that is provided by its internal environment and set by $U_{HT}(T)$.

These transformations from dQ/dt to an exit flux of information are allowed by the 2nd Law. This seemed to be a paradox for classical thermodynamics, but in this many-body quantum system it is allowed. It is also worth noting that the 'classical' arrow of time no longer exists in these transformations. Time is however now central with the new focus on dual capacitances in general, and to better understanding of why our oceans are getting hotter at ever faster rates. Time and energy together are central to a full understanding of quantum thermodynamic systems. The excitations in only one of our two energy capacitances display a finite range of lifetimes with a mean [6], as those that make up $C_{EX}(T)$ are not annihilated inside pure, defect free matter.

FTIR instruments used in studies of emitted spectral intensities

We have set up two types of instruments in our laboratory and applied them to studies of emitted spectral intensities from heated samples at a range of controlled T values and surface structures, over an almost full range of emission directions θ, for two polarisations. The first set-up used was in effect a thermal radiation directional emissometer $\boxdot\alpha$ A later approach [34, 37] used a different goniometer arrangement on which was mounted a heated sample. Data analysis described and tabulated in those reports includes direct colour maps of emitted and externally reflected spectral intensity as a function of direction and polarisation. The reflected intensities were used at that time [34], to find the Kirchhoff-Planck hemispherical emittance. This FTIR instrumentation was able to supply a full set of $I(\lambda,T)$ intensities emitted across most of the exit hemisphere from heated planar solids

and coatings with smooth and roughened interfaces. These instruments cannot however supply data for water so for it published, remotely sensed FTIR spectra were relied on to validate our predicted output spectral intensities. Transient temperature optical and thermal data over various time scales will be needed to observe the impacts of the internal energy component that is 'hidden' in equilibrium.

Heat build-up in landscapes

Modification of heating and cooling rates of landscapes and oceans by rising $C_{EX}(T)$ values are expected. Both will influence climate responses over time. Silica bonding is abundant in landscapes and many remotely sensed optical spectral intensities $I(\lambda,T)$ at infra-red wavelengths can be modelled with eqn.[4] using the observed refractive index wavelength profile for silica and silicon dioxide [7, 9]. Extending the hybrid pair models used to define the energy stored in water to storage in silica at 300K led to its $\varepsilon_H(T) = 0.157$, for a near surface optical amplification factor of ~6.4 so $C_{EX}(T) = 38{,}800$. Silica's $C_{HT}(T) = 750$ is less than the heat capacity of water by a factor of 5.6. Convective cooling by winds and evaporative cooling also influence environmental heating and cooling rates, and dT/dt. Landscape materials are diverse but based on silica studies we expect that the rate they store energy will also accelerate and will continue to do so while atmospheric intensities continue to rise.

ORCID iDs

G B Smith https://orcid.org/0000-0002-6985-2880

References

[1] Li Z, England M H and Groeskamp S 2023 Recent acceleration in global ocean heat accumulation by mode and intermediate waters *Nat. Commun.* **14** 6888
[2] Cheng L *et al* 2023 Another year of record heat for the oceans *Adv. Atmos. Sci.* **40** 963–74
[3] Ashcroft N W and Mermin N D 1976 *Solid State Physics: Holt* (Rinehart and Winston)
[4] Willrath H and Smith G 1980 A new transient temperature emissometer *Sol. Energy Mater.* **4** 31–46
[5] Hale G M and Querry M 1973 Optical constants of water in the 200 nm to 200 μm wavelength region *Appl. Opt.* **12** 555–63
[6] Smith G B, Gentle A R and Arnold M D 2022 Partial coherence and amplified internal energy when thermal radiation is sourced within matter *J. Phys. Commun.* **6** 065004
[7] Wenrich M L and Christensen P R 1996 Optical constants of minerals derived from emission spectroscopy: application to quartz *Journal of Geophysical Research: Solid Earth* **101** 15921–31
[8] Sova R M, Linevsky M J, Thomas M E and Mark F F 1998 High-temperature infrared properties of sapphire, AlON, fused silica, yttria, and spinel *Infrared Phys. Technol.* **39** 251–61
[9] Kischkat J *et al* 2012 Mid-infrared optical properties of thin films of aluminum oxide, titanium dioxide, silicon dioxide, aluminum nitride, and silicon nitride *Appl. Opt.* **51** 6789–98
[10] Friedel J 1956 On some electrical and magnetic properties of metallic solid solutions *Can. J. Phys.* **34** 1190–211
[11] Anderson P W 1978 Local moments and localized states *Rev. Mod. Phys.* **50** 191
[12] Smith D and Smith G 1971 s− d Exchange integrals obtained from experiment in Cu: Mn, Ag: Mn, and Au: Mn *Physical Review* B **4** 191
[13] Smith D and Smith G 1970 The high temperature properties of transition metal alloys *J. Phys. C: Solid State Phys.* **3** S69
[14] Smith G, Ben-David A and Swift P 2001 A new type of TiN coating combining broad band visible transparency and solar control *Renewable Energy* **22** 79–84
[15] Granqvist C G 2007 Transparent conductors as solar energy materials: a panoramic review *Sol. Energy Mater. Sol. Cells* **91** 1529–98
[16] Granqvist C G and Hultåker A 2002 Transparent and conducting ITO films: new developments and applications *Thin Solid Films* **411** 1–5
[17] Bilokur M, Gentle A, Arnold M, Cortie M and Smith G 2019 High temperature optically stable spectrally-selective Ti1-xAlxN-based multilayer coating for concentrated solar thermal applications *Sol. Energy Mater. Sol. Cells* **200** 109964
[18] Valkonen E, Karlsson T and Karlsson B 1983 editors . Selective transmission of thin TiN-films *Thin Film Technologies I* (SPIE)
[19] Bilokur M, Gentle A, Arnold M, Cortie M and Smith G 2015 editors. Optical properties of refractory TiN, AlN and (Ti, Al) N coatings *Micro+Nano Materials, Devices, and Systems* (SPIE)
[20] Landauer R 1961 Irreversibility and heat generation in the computing process *IBM J. Res. Dev.* **5** 183–91
[21] Santamouris M, Synnefa A and Karlessi T 2011 Using advanced cool materials in the urban built environment to mitigate heat islands and improve thermal comfort conditions *Sol. Energy* **85** 3085–102
[22] Smith G B and Granqvist C-G S 2010 *Green Nanotechnology: Solutions for Sustainability and Energy in The Built Environment* (CRC Press)
[23] Planck M 2012 *Eight Lectures on Theoretical Physics: Courier Corporation*
[24] Planck M 1914 *The Theory of Heat Radiation, English translation* ed M Morton P (Blakiston's Son & Co)
[25] Planck M 1914 *The Theory of Heat Radiation* (Blakiston)
[26] Brubach J-B, Mermet A, Filabozzi A, Gerschel A and Roy P 2005 Signatures of the hydrogen bonding in the infrared bands of water *J. Chem. Phys.* **122** 184509
[27] Querry M R, Holland W E, Waring R C, Earls L M and Querry M D 1977 Relative reflectance and complex refractive index in the infrared for saline environmental waters *J. Geophys. Res.* (1896-1977) **82** 1425–33
[28] Cheng J and Liang S 2013 Effects of thermal-infrared emissivity directionality on surface broadband emissivity and longwave net radiation estimation *IEEE Geosci. Remote Sens. Lett.* **11** 499–503
[29] Warren S G, Wiscombe W J and Firestone J F 1990 Spectral albedo and emissivity of CO_2 in Martian polar caps: model results *Journal of Geophysical Research: Solid Earth* **95** 14717–41

[30] Snyder W C, Wan Z, Zhang Y and Feng Y-Z 1998 Classification-based emissivity for land surface temperature measurement from space *Int. J. Remote Sens.* **19** 2753–74
[31] Seemann S W, Borbas E E, Knuteson R O, Stephenson G R and Huang H-L 2008 Development of a global infrared land surface emissivity database for application to clear sky sounding retrievals from multispectral satellite radiance measurements *Journal of Applied Meteorology and Climatology* **47** 108–23
[32] Hu S *et al* 2020 Deep-reaching acceleration of global mean ocean circulation over the past two decades *Sci. Adv.* **6** eaax7727
[33] Tai M C *et al* 2022 Spontaneous emergence of optically polarizing nanoscale structures by co-deposition of aluminum with refractory metals: implications for high-temperature polarizers *ACS Appl. Nano Mater.* **5** 4316–24
[34] Estherby C A, Arnold M D, Tai M C and Gentle A R 2021 Dynamic control of polarized thermal emission from VO 2 nanofins *Journal of Photonics for Energy* **11** 042111
[35] Sasaki S, Kou H, Masuda H and Kiyohashi H 2003 Total hemispherical emissivity of glass sheets with different thicknesses measured by a transient calorimetric technique *High Temperatures-high Pressures - High Temp-High Press* **35-6** 303–12
[36] Kish L B and Granqvist C G 2012 Energy requirement of control: comments on Szilard's engine and Maxwell's demon *Europhys. Lett.* **98** 68001
[37] Gentle A, Tai M, White S, Arnold M, Cortie M and Smith G 2018 editors. Design, control, and characterisation of switchable radiative cooling *New Concepts in Solar and Thermal Radiation Conversion and Reliability* (SPIE)